RESEARCH

Assessing the status of air pollution related to traffic using dispersion modeling: the case of Megenagna, Addis Ababa, Ethiopia

Bimrew Bizualem[1] · Kenatu Angassa[1] · Nurelegne Tefera Shibeshi[2] · Gudina Legese Feyisa[3]

Abstract

In emerging countries' expanding megacities, traffic is currently the main source of air pollution. Vehicles are the primary source of air pollution in Addis Ababa, the capital city of Ethiopia, because of the unimproved age of cars and bad road conditions. One of the city's major hub squares, Megenagna (between the Bole and Yeka sub-cities of Addis Ababa), has six significant road crossings that clog up traffic. The purpose of this study was to evaluate and forecast air pollution levels in the Megenagna region using the dispersion model (AERMOD). A sample campaign was run for 2 months (January and February) at 43 sampling stations. Hand-held Air-test Model-CW-HAT2005 and Aeroqual series 5000 devices were used to measure gaseous pollutants (SO_2 and NO_2) and particulate matter ($PM_{2.5}$ and PM_{10}). There is a lot of spatial variation throughout the study site, as shown by the statistically significant difference between sampling locations ($p < 0.05$). The sensitivity variation of 1 m/s and the 45° wind direction with respect to the horizontal of the receptor of the self-monitored sample location were ideal for the prediction, calibration, and validation of pollutants in AERMOD. It was anticipated that gaseous and particulate pollution would vary from site to site, with SO_2 exceeding the threshold. This study demonstrates the need for additional research into the spatiotemporal variance of emissions due to traffic in Addis Ababa.

Keywords Dispersion model · Gaseous pollutants · Particulate matter · Traffic air pollution

✉ Kenatu Angassa
    kenatuangassa@gmail.com

1   Department of Environmental Engineering, College of Engineering, Sustainable Energy Center of Excellence, Addis Ababa Science and Technology University, Addis Ababa, Ethiopia

2   School of Chemical and Bioengineering, Addis Ababa University, Addis Ababa, Ethiopia

3   Center for Environmental Sciences, Addis Ababa University, Addis Ababa, Ethiopia

1 Introduction

Indoor air pollution causes the majority of air pollution in Africa (Piqueras and Vizenor 2016; Dida et al. 2022). Carbon monoxide, carbon dioxide, gaseous pollutants, and other primary pollutants are released into the environment when charcoal is burned uncontrollably and used as fuel for various purposes, such as food preparation (Abera et al. 2021) (Obanya et al. 2018). Today, vehicle transportation is also recognized as a significant contributor to air pollution in newly developing megacities (Nieuwenhuijsen 2016; Singh et al. 2021; Haslina et al. 2022); this contributes to both immediate health effects and future climate change (Caserini et al. 2013; Takuchev et al. 2014).

The African Union's (AU) conference headquarters are located in Addis Ababa, the capital of Ethiopia and one of the continent's emerging megacities (Habtamu. 2020). Urbanization and industrialization are growing alarmingly quickly today (Addis Ababa urban planning report, 2018) due to this people migrate from rural to the city. As a result, a strong annual population increase rate was seen, with an estimated 4.79 million people in the 2017 census (UN 2017). This has directly raised the demand for the city's transportation system (Kume et al. 2010). The total number of vehicles was 8264 in 2005, and there were three times as many automobiles in 2015 as there were in 2005 due to significant investment in the transportation and other services industries (Wondifraw 2019). According to the Addis Ababa Transport Authority report from 2016, the city's annual growth rate for imported vehicles is 9.88%. Air pollution caused by traffic is now a serious issue in Addis Ababa (Fekadu 2017). Another obstacle to reducing traffic-related air pollution is the main driver of increased long-distance travel (Kumie et al. 2021), improper maintenance of older vehicles, and slowly expanding road networks and design (Kebede et al. 2022).

According to the United Nations (2017), Megenagna is one of the cities of Addis Ababa's main gathering places where most people congregate to exchange goods and services, travel in various directions, and communicate. People are sensitive to exposure to traffic air emissions due to mixed (transport and population) enormous amounts of transportation systems. Because of the extreme traffic congestion in the street and Megenagna Square, there is a serious problem with this traffic-related air pollution. It is critical to assess the effects of receptor exposure because it is difficult to accurately predict how pollutants will disperse in this dispatch region given the current traffic situation. Since air pollution is the primarily distributed contaminant, it is challenging to numerically analyze and make precise predictions (Mehrdad. 2013).

Basic dependent and independent input variables for the ADMs model include meteorological, emission rate, topography data, building, and elevation data (Sunil et al.,2015). The most popular model is the USEPA-approved American Environmental Regulatory Model (AERMOD), which relies on steady-state conditions, continuous emission, and environmental considerations (US EPA 2015). Indicating the line source model with the mixing of pollutants in line, line-area, and line-volume circumstances is another application of the AERMOD (Wei et al. 2016). In determining the emission rate, this dispersion model was employed (Milando and Batterman 2018) and was developed (Wang et al. 2008) (Equation (1)).

$$C = \frac{Q}{2\sqrt{2\pi}\delta_{zue}}\left[\exp\left\{-\frac{1}{2}\left(\frac{z-h_o}{\delta_z}\right)2\right\} + \exp\left\{-\frac{1}{2}\left(\frac{z+h_o}{\delta_z}\right)2\right\}\right]$$

$$\times\left[\mathrm{erf}\left|\frac{\sin\theta\left(\frac{L}{2}-y\right)-x\cos\theta}{\sqrt{2}\delta_y}\right| + \mathrm{erf}\left|\frac{\sin\theta\left(\frac{L}{2}+y\right)+x\cos\theta}{\sqrt{2}\delta_y}\right|\right] \tag{1}$$

where C stands for the pollutant concentration ($\mu g/m^3$), Q for the emission rate per unit length (g/m.s), ue for the effective wind speed (m/s), $h0$ for the plume center height (x from the road) distance (m), and z for the receptor's height above the ground (m). Pollutant's y and z are the standard deviations in a crosswind's horizontal and vertical directions (m). L is the length of the source (in meters), h is the angle between the ambient wind and the road, erf is the error function, x is the receptor's distance from the source line (in meters), and y is the receptor's distance from the centerline of the road together with the source line (m). The total emission of the pollutant (Ep) for each source is estimated by the model as Equation (2) (Kumar et al. 2016).

$$\text{Ep} = \sum_{i=0}^{n} \left(e_{ip}(V) \times Ni \right) L, \tag{2}$$

where $e_{ip}(V)$ is the emission factor for pollutant p and vehicle class I as a function of average speed V; Ni is the number of vehicles of class I; and L is the length of the road segment. The emission rate is also influenced by the average speed, the mass of the vehicle, and the technology used to reduce emissions.

It is crucial to properly aggregate cars by classes and categories to obtain an accurate estimate of air pollutant emissions (Caserini et al. 2013). To improve the simulated data, the sensitivity test and data validation are used (Kerr et al. 2014). The simulated data are improved by using dispersion modeling to model and validate concentration in various scenarios for the second independent variable (Bachtiar et al. 2020). To solve Addis Ababa city's poor air quality issue and provide an explanation to the regulatory authority, monitoring, and forecasting traffic-related pollution is crucial. As a result, this study was an oversight of the use of AERMOD to measure the dispersion of traffic-related air pollution in Megenagna, Addis Ababa, over a 1.5 km by 1.5 km region.

2 Methods

2.1 Description of the study areas

The city of Addis Ababa, the capital of Ethiopia, which is located at 8° 55′ N, 38° 45′ E, was the site of this study. Addis Ababa City is around 20 km long from north to south and about 25 km long from east to west. It is located between longitudes 380 43′ and 380 50′ east and latitudes 80 56′ and 90 05′ north. The Megenagna region of Addis Ababa, which is halfway between Bole and Yeka, was chosen as the study location. According to their respective densities of 5165.1 and 3190.7 people per square kilometer, Yeka and Bole's sub-cities have a total population of 424,217 and 378,104, respectively (Aklilu and Necha 2018).

2.2 Site selection

The six road lines of Megenagna that are shown in Fig. 1a, the sampling station, are where the sampling points were chosen. Megenagna has two main rings (R1 and R2) in the station, and the sample was collected in two different ways, namely at a root sample site near the bus station areas and on a road line outside of the root. The entrance of Bole-Goro road (Ring road), CMC road, Meskel square road, and Kenenisa road are all found in the first square (R1), which is situated in the lower elevation (Kenenisa Avenue). The second square
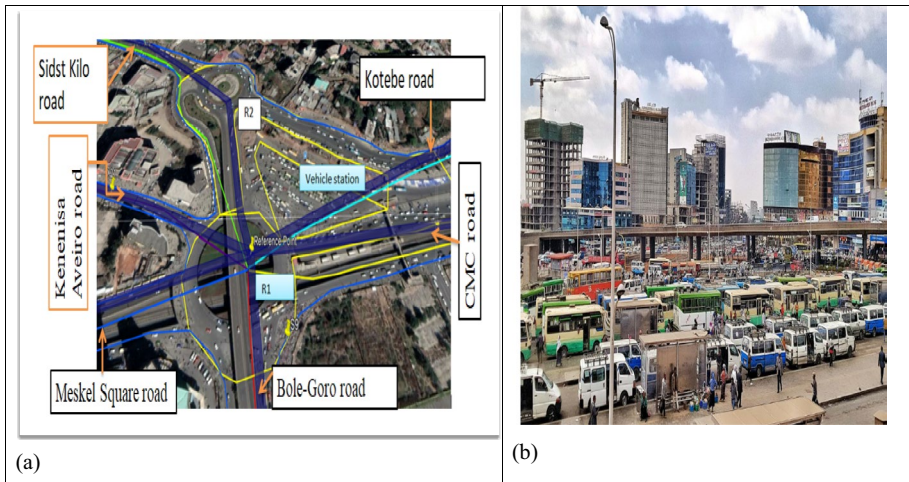
Fig. 1 Sampling station. **a** Root sample site and **b** bus station (source: Google Earth Pro 2.3)

(R^2) is situated above the bridge entrance of Bole-Goro road (Ring road) and Asmara road, at the upper station of Megenagna, which connects Sidst Kilo road (Fikremariam Aba Techan str.) and Sidst Kilo road (Kotebe road). Further line source samples were collected at each intersection of the road that leads away from Megenagna's root. Images of the bus station's traffic flow can be seen in Fig. 1b. There were 43 sample locations, 16 of which were taken in the bus terminal, and the remaining 27 sampling points were occupied along each road line while taking into account the concentration of road sensitive points.

Table 1 lists the 27 sampling locations from the six road lines, which are, in order, road 1 (Six-Kilo Road Line), road 2 (Kenenisa Avenue Road Line), road 3, (Meskel square road line), road 4 (Bole-Goro Road Line), road 5 (CMC Road Line), and road 6 (Kotebe Road Line).

2.3 Sample collection

Over the study period, data from various scenarios, both qualitative and quantitative, were gathered. The sampling period ran from January 1 to February 28, 2021. Ethiopia is currently experiencing its dry season. The first month's sample, January, was utilized for model simulation and calibration, while the second month's sample, February, was used for model validation by cross-monitoring of the first sample points. Three peak hours morning, noon, and afternoon were chosen for sample measurement. To cover sample measurement at all of the chosen sample points during sampling, both transit walk and transport systems were employed. The street stands' average height of 1.5 m was used for the sample analysis because that height is what is advised for human respiratory intake.

$PM_{2.5}$ and PM_{10} aerodynamic diameters were measured on the field using Air-test portable sensing equipment (Model-CW-HAT2005). The portable Air-test sensor was created to measure the $PM_{2.5}$ and PM_{10} concentrations in the air for 60 s at a 500 mL flow rate using the accepted methodology (Lin et al. 2015). On the other hand, gaseous pollutants (SO_2 and NO_2) were measured using Aeroqual (Model Series 500 (2016)) within the same port in the various sensors. All of the vehicles that went by the sample points during the busiest

Table 1 Sample point, the distance between the sample point, and respective coordinate

Sample station	Distance between sample points (m)	Coordinates	
		UTMX	UTMY
R	0	478,214.3	997,033.6
Sr_1	80	478,456	997,068.4
Sr_2	67.5	478,448.1	997,121.1
Sr_3	89	478,379.4	997,068.3
Sr_4	67.2	478,381.8	997,080.9
Sr_5	68	478,314.7	997,137.6
Sr_6	65	478,292.7	997,112.2
Sr_7	65.5	478,260.2	997,080
Sr_8	45.5	478,276.9	996,980.9
Sr_9	68	478,269.6	996,978.7
Sr_{10}	70	478,281.1	997,009.9
Sr_{11}	49.5	478,176.4	997,044.4
Sr_{12}	46.5	478,241.7	997,089.5
Sr_{13}	63.25	478,263.7	997,114.6
Sr_{14}	57.5	478,251.7	997,192.4
Sr_{15}	105	478,185.1	997,246.6
Sr_{16}	58.5	478,157.6	997,187.7
S_{11}	146	478,093	997,333.4
S_{12}	233	477,991.6	997,335.9
S_{13}	345	477,701.4	997,520.3
S_{14}	335	477,586.9	997,520.7
S_{15}	332	477,046.3	997,592.6
S_{21}	267	478,042.9	997,905.3
S_{22}	306	477,906.3	997,103.2
S_{23}	258	477,533.9	997,132.9
S_{24}	281	477,444.7	997,162.7
S_{25}	388	476,770	997,189.5
S_{31}	373	478,031.9	998,478.9
S_{32}	360	477,709.3	996,939
S_{33}	352	477,503.8	996,902.6
S_{34}	376	477,435.4	996,837.5
S_{35}	227	477,991.6	997,335.9
S_{41}	165	478,255.7	996,814.9
S_{42}	268	478,214.6	996,914.8
S_{43}	156	478,301.2	996,810
S_{44}	365	478,450.2	996,726.7
S_{51}	234	478,982.5	997,067.6
S_{52}	454	479,698.1	997,113.9
S_{53}	521	478,474.1	997,024.9
S_{61}	160	478,637.6	997,156.8
S_{62}	348	479,338.6	997,223.4
S_{63}	373	479,538.2	997,191.1
S_{64}	277	478,093	997,333.4

Sr is the root sampling point in the bus station area. Whereas, S_{1n}, S_{2n}, S_{3n}, S_{4n}, S_{5n}, and S_{6n} represent the sample points in the six road lines, with n describing the index of the sample point in each sample station

time of the day were counted. Cars were divided into heavy-duty, medium-duty, and light-duty categories for the study. Overall, the Air-test instrument (Model-CW-HAT2005) and Aeroqual are both effective tools for measuring particle and gaseous contaminants Table 2.

2.4 Data analysis and model setup

2.4.1 Data analysis

The average concentrations of each parameter were used as input for the AERMOD software after the raw data was compiled and summarized using an MS Excel sheet. The average daily traffic (ADT) and average monthly traffic (AMT) were calculated and examined, together with the traffic flow at the sample places, wind speed, wind direction, surface temperature, meteorological temperature, and wind speed. Results were compared to the recommended value, which was established by the Ethiopian Environmental Protection Commission and WHO's 24-h air quality monitoring.

2.4.2 Meteorological data preparation

The meteorological agency supplied the metrological information, which included the following variables: temperature, relative humidity, cloud cover, precipitation, wind speed, and wind direction. A site-based air test sensor also measured temperature and relative humidity in addition to these facts. To assess its impact on the level of pollution in the research locations, meteorological data was employed as an independent variable. Since meteorological factors are the primary element determining the dispersion of emissions in the ambient environment, the impact of climatic variables such as wind speed and wind direction was highlighted to assess the condition and extent of air pollution in Megenagna (Bachtiar et al. 2020). Using WRPLOT view 9.8 to locate the eight directions of wind flow in the east, west, north, or south as well as the corresponding nearby direction of the wind in the study areas, the wind rise was calculated. The meteorological bureau provided data for the 2 months' variation in wind speed and wind direction during the day.

The colorful legend in Fig. 2a depicts how often wind speeds are present in the indicated direction. A wind rise shows wind direction and frequency in the Megenagna region. In the Megenagna region, a wind rose shows wind speed and direction frequently. The majority of wind probabilities were in an east-to-west direction rising at a 248° bend. The majority of wind direction predominated to the west at Megenagna bus station, and the percentage contribution of wind speed was 41%. Maximum wind speeds more than or equal to 11.1 m/s were frequently reported, while minimum speeds of 0.5 m/s were as well.

Table 2 Detection threshold, the data range, and some characteristics of the Air-test instrument (Model-CW-HAT2005) and Aeroqual (McKercher et al. 2017)

Instrument	Pollutants	Detection threshold	Data range
Air-test instrument (Model-CW-HAT2005)	$PM_{2.5}$	0.1 μg/m³	0 to 1000 μg/m³
Air-test instrument (Model-CW-HAT2005)	PM_{10}	0.5 μg/m³	0 to 1000 μg/m³
Aeroqual portable monitor	SO_2	0.1 ppb	0 to 500 ppb
Aeroqual portable monitor	NO_2	0.1 ppb	0 to 500 ppb
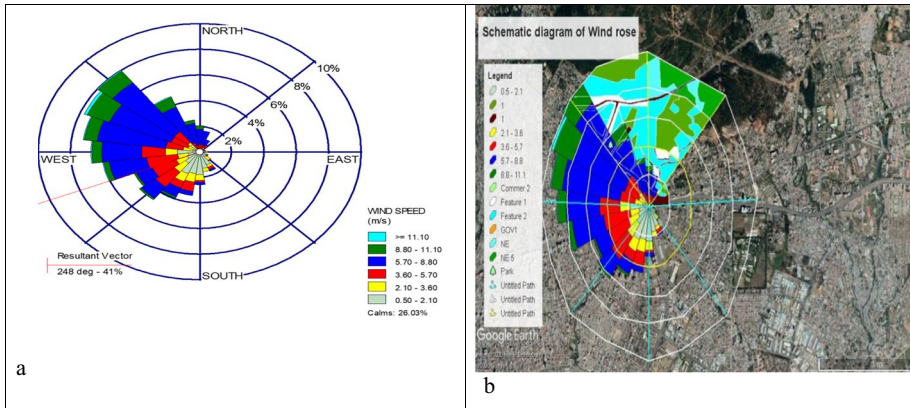
Fig. 2 **a** Wind rose in January and February and **b** dominant of wind rose in sample location

In Fig. 2b, buildings were classified according to their height as highest, medium, and small, ≥ 30 m, 15 m $\leq b < 30$ m, and <15 m, respectively. The length of the buffer zone from the major road was estimated. The sample point's elevations as well as the demographics of the Yeka and Bole sub-cities per-residence density were used as inputs. Using WRPLOT software on top of Google Earth Pro, the primary preset meteorological variables of wind speed and wind direction were added as the independent variable.

2.4.3 Model setup

Using AERMOD software, an observational study of air pollution concentration was replicated. There are five paths in AERMOD's environmental system. They are the output pathway, meteorological pathway, source pathway, and control pathway. The steps for operating AERMOD were sequential. The new project was launched at its focal point (47,723.20, 997,169.40) using the World Geodetic 1984 projected 1.5 km by 1.5 km coordinate system in the 37N universal time zone. In the source route, a template format for the first stage impact of the parameter from the Excel sheet was created in the chosen station of line source ID. Average building height, width, and cross-flow were taken into consideration in the second step of the source pathway. In the source route, a template format for the first stage impact of the parameter from the Excel sheet was created in the chosen station of line source ID. Average building height, width, and cross-flow were taken into consideration in the second step of the source pathway. Maximum hourly background concentration is assessed at the starting and finishing numbers for further validation purposes. Except for the reference point in the root, this pathway's base elevation (0 m) and road width were measured in increments of 20 to 30 m. With 43 sampling points and a user-specified average human height of 1.5 m, the number of receptors on the receptor pathway is identical to the number of receptors allocated by default. Starting at the root of Megenagna, the distance between receptors was estimated to be 25.5 m. The terrains chosen were flat, raised, and uniformly Cartesian. AERMET software was employed on the meteorological pathway as an independent variable of the AERMOD input value. Surface file (SFC) and profile file (PFL) formats were utilized as the result of AERMET meteorological preprocessing of the data. From the archived data file, the raw met data was taken out and organized. Twelve-hour data were retrieved from a 24-h collected data file. For the AERMET input

data file, all required data files were prepared. Wind speed, wind direction, relative humidity, precipitation, dry temperature, and cloud cover were the primary variables that AERMET processed.

Eventually, the output of the AERMET program contains one or more levels of the profile of wind speed, wind direction, temperature, and standard deviation of the fluctuation component of the wind. The surface data file (sfc) is utilized for boundary layer scaling parameter height of wind and temperature. The counter profile as it had been automatically generated by AERMOD was examined. The entire procedure from the projection to the metadata was double-checked on the output pathway. The last step is run before determining whether the progression is successful, and the run is then verified using the message's instructions for the error and warning messages.

In the AERMOD software environment, the model's output is executed in three-time intervals for a chosen control hour (rush time, morning, and afternoon). The plot AERMOD was used to predict particulate matter and gaseous pollutants from vehicle emissions for average time options of 3, 6, and 12 h. These times were chosen because they represented the traffic's peak. Pollutant concentration and dispersion are influenced by the contour line; the higher the contour line, the higher the concentration of pollutants. The first scenario must represent the period from 1:00 to 3:00 AM local time, and the second scenario must represent the average of 6 h from 1:00 to 6:00 AM. Typically, incoming data processes a variable to produce an outcome, as seen in Fig. 3. According to the color-coded legend with the concentrations of contaminants, simulations of certain concentrations were done. According to the contour line surface simulation for the categorization in the AERMOD environment, there was a considerable amount of pollution.

2.5 Calibration and validation of the model

The model evaluation is required to raise the level of trust in the observed data before the research findings are reported for a decision-maker to implement the socio-economic implications of air pollution. Model prediction requires research findings after the examination of statistical analysis. Different calibration techniques have an impact on the sensitivity change as the independent variable changes. The expected concentration, the dependent
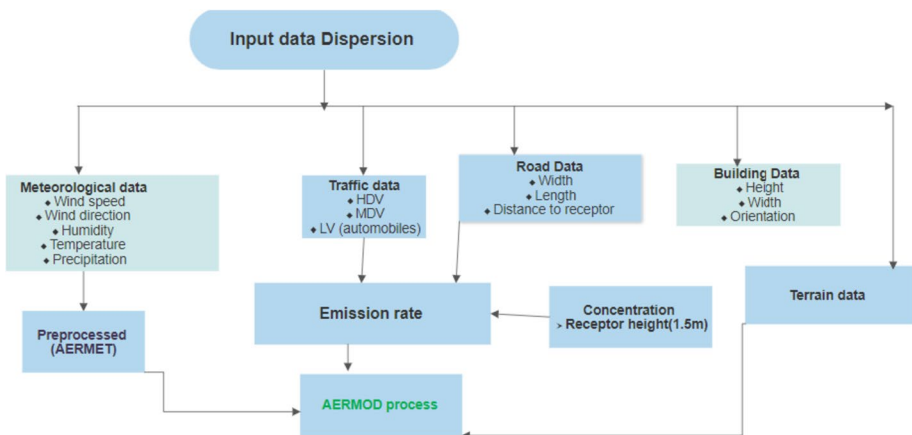

Fig. 3 Model setup and data analysis

variable, and the observed value were contrasted. The model was then tested using the final set of simulated data for the second-month data. As one variable was checked, the simulation's first value was compared to the data that had been collected. The projected value was simulated in various ways by altering the independent variable of the metadata value while keeping the dependent input variable fixed. In comparison to relative humidity and precipitation, wind speed and wind direction were chosen for model testing since they are the key factors impacting the dispersion of pollutants during the dry season (US EPA 2003).

Dispersion modeling was used to simulate the investigation modeling and validation of PM10 concentration. This was done twice for the sample that was collected (Bachtiar et al. 2020). The second sample was used to validate the pollutants while the first sample was utilized to simulate PM_{10} at the default values of 0°, 30°, and 60°. In terms of traffic volume and density, the angle of $0° < a < 90°$ revealed the highest concentration of PM_{10}, with 61% and 51%, respectively. This first thought led to the validation of the research utilizing a try-and-error value adjustment of the dependent and independent variables of wind speed and wind direction with the concentration outcome in the January and February data.

3 Result and discussion

3.1 Dispersion of particulate matter (PM)

The contour line determines the dispersion and concentration of contaminants; the higher the contour line, the more pollutants are present. The highest simulated value was displayed in a significant level red color with a high contour line, while the lowest concentration was displayed in a violet color with a lower contour line. To adjust the multiplication factor of the result in the AERMOD environment, the emission rate for the output pathway was employed as a user-defined factor of 10. The pink color was anticipated to have the lowest value far from the Megenagna root, while red was predicted to have the highest value close to it. To foretell the concentration difference in the peak hour variation, the AERMOD simulation was given the go-ahead. The first 3-h average of $PM_{2.5}$ was expected to have a maximum concentration of 34.8 µg/m^3 and a minimum concentration of µg/m^3, as illustrated in Fig. 4a. The highest and lowest predictions for the first average 6-h $PM_{2.5}$ concentration were 34.9 µg/m^3 and 0.7 µg/m^3, respectively.

The projected maximum and minimum PM_{10} concentrations for the first 3 h were 68.8 µg/m^3 and 0.7 µg/m^3, respectively (Fig. 4b). According to Table 3, the maximum and minimum expected PM_{10} concentrations for the 6-h concentration were 63.3 and 1.0 µg/m^3, respectively, while for the 12-h prediction, the maximum predicted concentration was 40.6 µg/m^3 and the lowest predicted concentration was simulated at 0.4 µg/m^3. The maximum predicted values for the first 24-h average from area, line, and point sources were 339 µg/m^3, 24 µg/m^3, and 11 µg/m^3, respectively, in the investigation on PM_{10} dispersion model prediction that was carried out in the high-rise metropolis (Onat 2016). The line source model's predicted concentration of PM_{10} was lower than the actual results. This could be a result of the traffic intensity or the difference in time. In cities in India and the UK near roads, a comparison of the dispersion model of $PM_{2.5}$ was conducted (Gulia et al. 2015). It was predicted that Delhi, Chennai, and Newcastle city will have first-hour average $PM_{2.5}$ concentrations of 114.14 µg/m^3, 87.10 µg/m^3, and 14.26 µg/m^3, respectively. In comparison to the current findings, Delhi and Chennai had a
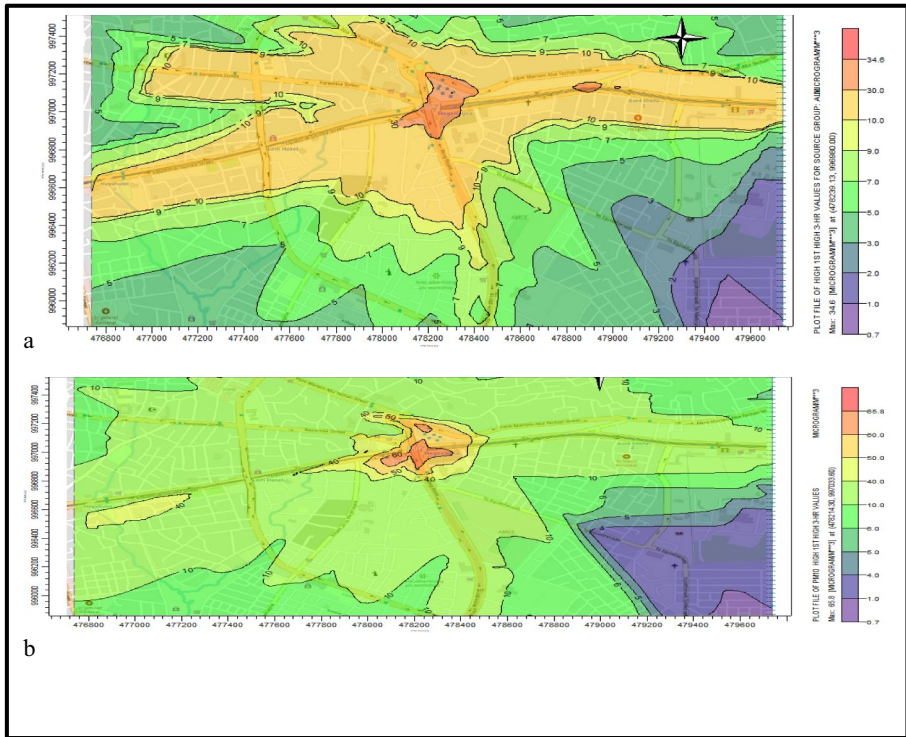
Fig. 4 Prediction of PM in the first 3-h average: **a** PM$_{2.5}$ and **b** PM$_{10}$

Table 3 Prediction of PM in different scenarios

| Parameters	Prediction (simulation)	3-h average	6-h average	12-h average
PM$_{2.5}$	Maximum	34.81	34.9	29.9
	Minimum	0.7	0.4	0.2
PM$_{10}$	Maximum	68.8	63.3	40.6
	Minimum	0.7	0.6	0.4

larger concentration of projected value, while Newcastle city had a lower concentration and lower relatively with Newcastle city.

The highest predicted concentration of PM was observed in the first hour of an average 3-h scenario. The lowest PM concentration was projected in the lower contour line of the violet color, which is away from the bus station, while the highest PM concentration was typically expected in the middle of Megenagna with a high contour line. The largest expected amount of pollutants was predicted to disperse in the southwest, upwind, for the first average of 3 h. It includes emissions from a wide range of close-by traffic. The line source model underestimated oblique and crosswind conditions while overestimating parallel wind direction in the other area of investigation (Goyal and Dhir 2015).

3.2 Prediction of gaseous pollutants

A new spatiotemporal variation was used to forecast the dispersion of gaseous pollutant concentration. During the day's busiest time, notably early in the morning, the automobile count revealed the highest traffic flow. The model was to simulate the concentration of gaseous pollutants with peak hour emission in the first 3-h, 6-h, and 12-h scenarios, depending on the source's emission inventory. In the AERMOD setting, the initial average of 3, 6, and 12 h with a considerable amount of SO_2 concentration was simulated. According to the simulation in the red color at Megenagna's center, as seen in Fig. 5a, the first average 3-h maximum SO_2 prediction was 973.7 µg/m^3. Due to traffic density and prolonged idle times, pollutant dispersion is lower in the center. Because traffic signals and crossroads at this station affect the concentration level, the pink color was simulated between 700 and 900 µg/m^3 next to the Lam Hotel on the Meskel square road line. Together with the CMC road line's high traffic density, Fig. 5's large concentration of construction and maintenance equipment is also noticeable.

In the initial average 3-h simulation, as depicted in Fig. 5b, the greatest NO_2 prediction was simulated. NO_2 concentrations for the first average of 6 h were predicted to be 78.8 and 0.8 µg/m^3, respectively. The first average 6-h simulation indicated a moderately significant level of pollution, which was a minimal concentration. The AERMOD line source model of vehicular NO_x emission was created in a recent study (Amoatey et al. 2020). The first average of 3 h had the highest simulated NO_2 concentration level, which was measured at 188.22 µg/m^3 among the 24-h prediction. Due to Muscat's high traffic density, this number was larger than that found in the current study. Observation vs. prediction-fitting correlation coefficient
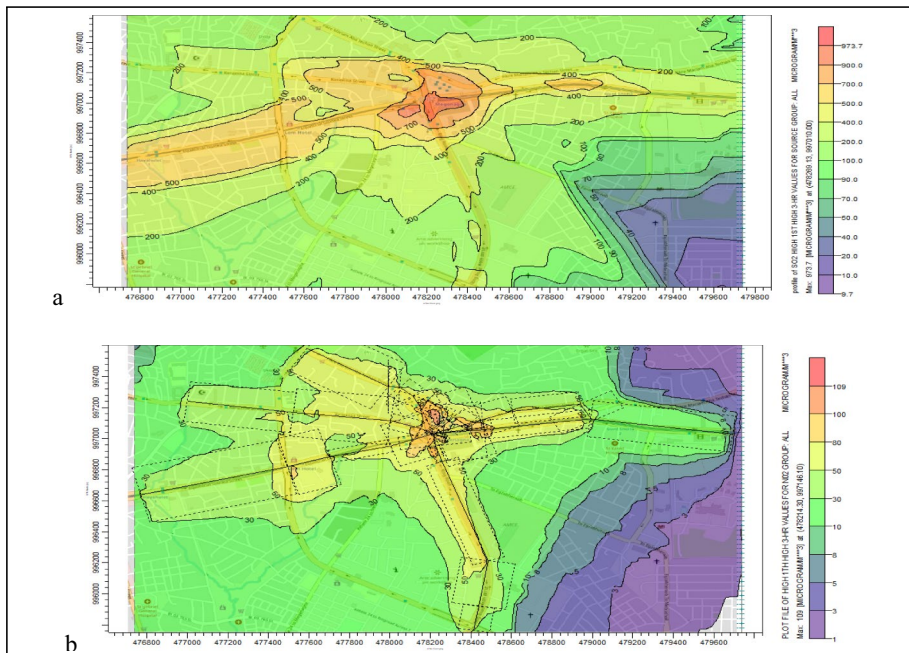
Fig. 5 First 3-h average predicted gaseous pollutants for **a** SO_2 and **b** NO_2

was used to assess the accuracy of the gaseous pollutant prediction. Perception of more than 88% of the fitting curve was found during the experiment. The correlation coefficients of NO_2 between predicted and observed values were $R^2 = 0.904$. This demonstrates that the simulated value was the best suited. A study of many studies revealed that in Sydney, the monthly and hourly value regression coefficients for SO_2 were $R^2 = 0.57$ and $R^2 = 0.34$, respectively (Gibson 2013). The regression coefficient of SO_2 in the preview study had the lowest fitting value compared to the results of the current study, which is consistent with those findings. This was caused by the variation in the finding's meteorological and spatial variability. The correlation coefficients for SO_2 and NO_2 varied from 0.73 to 0.96 and 0.73 to 0.95, respectively, when the general finite line source model employing the dispersion model was established (Kumar et al. 2016). This value shows the best fitting compared with the current study. The regression coefficient fits the data less well than the present result. This can be due to the distinction between metrological and geodemographic variability.

3.2.1 Sensitivity test and calibration of AERMOD

Different calibration techniques cause the sensitivity (the independent variable) to change and have an impact on the dependent variable. The value that was observed and the dependent variable were compared. As one variable was checked, the first value from the simulation was compared to the data that had been collected. The projected value was simulated in various ways by altering the independent variable of the metadata value while keeping the dependent input variable fixed. Because these characteristics have a greater impact on model predictions than relative humidity and precipitation during the dry season, they were chosen for model testing. As shown in Table 4, the five categories A, B, C, D, and E each had a distinct speed value; thus, the AERMOD software set the default value for each category to be constant.

The calibration process involved five steps of the category. The main prediction variable equation was created using wind speed or direction change, and the anticipated value was simulated as either a maximum or minimum value. As a substrate of wind speed and wind direction, the objective function (concentration) varied in various calibrations sensitivity changes from Equation (3). The influence of the receptor in the monitoring area was found to be sensitive; if the wind was blowing from the south or west, the impact of the receptor would become more pronounced in the other geographic location when the wind direction changed (Bachtiar et al. 2020).

$$Z1\ (Xi,\ Yi)\ =\ Q\ (aXi\ +\ bYi), \tag{3}$$

where $Z1$ is the predicted value due to the change in independent variables Xi and Yi, wind speed and wind direction, respectively. Q is the independent variable input value of emission rate and observed value, and a and b are the other constant values. The maximum and minimum value of pollutants was simulated in different wind speeds and wind direction variation as presented in Table 5. As indicated in Table 5, the regression values for SO_2 and NO_2 were $R^2 = 0.91$ and $R^2 = 0.96$, respectively, while the regression values for $PM_{2.5}$ and PM_{10} were calibrated and were $R^2 = 0.95$ and $R^2 = 0.93$, respectively.

Table 4 Calibration test of the AERMOD default value

Categories	A	B	C	D	E
Wind speed (m/s)	1.54	3.09	5.14	8.23	10.8
Wind direction (°)	0	0	0	0	0

Table 5 Model calibration using different scenarios

| Parameter		Wind speed/wind direction				
		Scenario-1	Scenario-2	Scenario-3	Scenario-4	Scenario-5
		Default/0^0	+_0.5/30^0	+_1/30^0	+_0.5/45^0	+_1/45^0
$PM_{2.5}$ (µg/m^3)	Max	33.5	33.8	34.6	32.6	34.9
	Min	0.1	0.2	0.7	0	0.4
PM_{10} (µg/m^3)	Max	40.6	63.6	64.3	45.4	65.8
	Min	0.4	0.6	0.2	0.5	0.7
SO_2 (µg/m^3)	Max	618.2	823.6	964.5	756.8	973.7
	Min	6.2	7.2	9.6	6.4	9.7
NO_2 (µg/m^3)	Max	116	163.6	85.8	63.6	109
	Min	4	3	0.7	0.6	1

3.2.2 Validation

Using the 2 months of collected data, the model's validity was developed. The data from the first month were utilized for model calibration and prediction, while the data from the second month, collected via self-monitoring at the same sampling locations, were used for validation. The second month of observed data was used as an input simulated model, with the independent variable of the simulated data remaining unchanged. The objective function simulation model was utilized for validation, except for the dependent variable used as a function of the concentration's self-monitored value for the second month, as shown in Equation (4).

$$Z_2(Qi) = aX(Ci) + bY(Qi) + \varepsilon, \tag{4}$$

where Z_2 is the concentration of output as the second-month emission rate imported, which maintains the independent variable constant optimum values (scenario-5) in calibrated models; Qi is the emission rate of pollutants; Ci is the concentration of the second-month cross-monitored; X and Y are the independent variables with the constant coefficient of a and b; and ε is an error.

The maximum concentrations of $PM_{2.5}$ and PM_{10} were 36.6 and 66.6 µg/m^3, respectively, with fitting values of regression analysis of 98% and 90%. While PM_{10} was somewhat lower than the monitoring value in Fig. 6, the validation of $PM_{2.5}$ was roughly the best fitting to the truth value of monitoring data. For $PM_{2.5}$ and PM_{10}, the estimated inaccuracy was 2% (0.02) and 10% (0.1), respectively. Around 90% of the anticipated validation of PM was accomplished. In the other study, simulations of dispersion modeling were used to model and validate PM_{10} concentration under various scenarios for the second independent variable (Bachtiar et al. 2020). For the collected sample, the analysis was done twice. The first sample was used to simulate PM_{10} at default values of 0°, 30°, and 60°, while the second sample was used to validate pollutants. At an angle of $0° < a < 90°$, the largest concentration of PM_{10} was found, with 61% and 51%, respectively, of the total traffic volume.
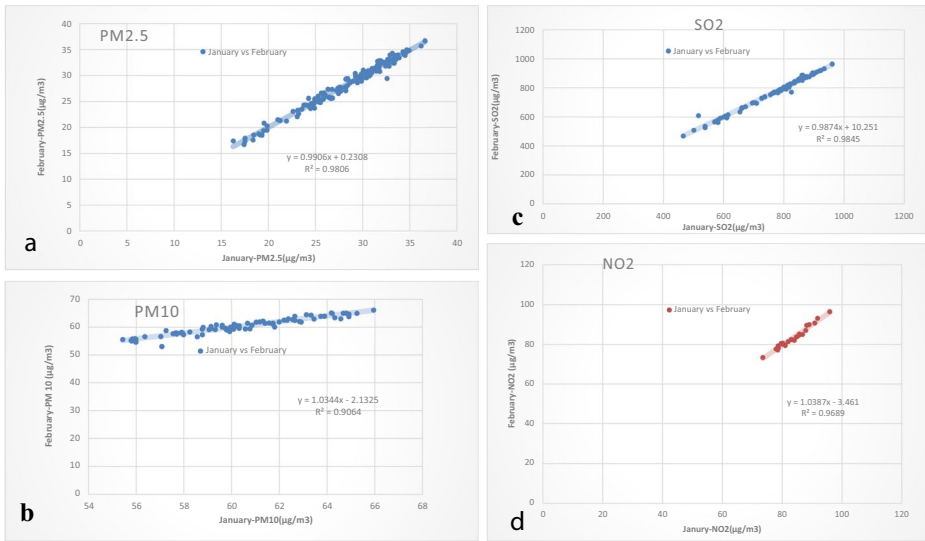
Fig. 6 Validations of data of **a** $PM_{2.5}$, **b** PM_{10}, **c** SO_2, and **d** NO_2

Around 95% of the calibrated validations for cross-monitoring gaseous pollutants were obtained. The perspective error was 2% (0.02) and 4% (0.04), respectively, with SO_2 and NO_2 fitting best at 98% and 96%, respectively. With the help of regression analysis, the task of estimating model validation of gaseous pollutants was completed to the best of fitting using the first month as simulation modeling and the second month for validation purposes.

Statistical modeling is essentially dependent on the evaluation of sampling points. Correlation, root mean square error (RMSE), bias, mean absolute error (MAE), mean bias error (MBE), and mean square error (MSE) statistical analysis methods were used to check and validate emission-related variables such as particulate matter and gaseous contaminants. Cross-validation of seen and predicted data is a technique used to assess a predictive model's performance on unobserved data. It entails repeatedly dividing the data into two sets: training and testing. The model is trained on the training data and then used to predict the test data. This process is performed several times with different data splits, and the model's average performance across all folds is calculated. The correlation between observed and predicted was best feted (0 to 1). In Table 6, RMSE values between 0 and 20% show that the model can relatively predict the data accurately. The lower value of RMSE indicated the best fit of the model. NO_2 indicated that the higher value implies that

Table 6 Cross-validation of observed and predicted data

Parameters	Efficiency						
	Correlation	RMSE	R^2	Pbias	MAE	MBE	MSE
$PM_{2.5}$	0.990	0.076	0.981	−0.021	0.006	−0.006	0.006
SO_2	0.992	0.082	0.985	0.001	0.009	0.009	0.007
PM_{10}	0.963	0.131	0.906	0.024	0.015	0.015	0.017
NO_2	0.919	1.042	0.968	0.250	0.208	0.208	1.086

cross-validation was not accurate. It might be the sensitivity of the model at NO_2 (1.042). The probability of bias also was the best result, while at $PM_{2.5}$, under-predicted results were obtained.

Generally, RMSE, bias, MAE, MBE, and MSE indicate a better fit between the observed and predicted data except for NO_2, which was higher at RMSE and MSE, with values of 1.042 and 1.086, respectively.

4 Conclusion

Assessment and forecasting of traffic-related air pollution in Megenagna, Addis Ababa, was the main conclusion of this study. The best calibration was obtained with a wind speed of 1.0 m/s at 450 with a higher probability of receptor. Air pollution prediction using AER-MOD reached over 75% of R^2 with monitored data. Except for SO_2, the concentration of both gaseous and particle pollutants in the Megenagna area did not exceed the regulatory guideline when the expected pollution level was compared to it. It may be necessary to evaluate the fuel type and automobile model because the gaseous pollutant SO_2 was significantly above the advised level. This research was only able to focus on the 2-month variation of January and February due to time and money constraints, but additional seasonal and geographical region coverage research is essential to address Addis Ababa's air pollution issues.

Data Availability Supporting data available in the manuscript

Declarations

Ethical approval and consent to participate Not applicable

Consent for publication Not applicable

Conflict of interest The authors declare no competing interests.

References

Abera A, Friberg J, Isaxon C, Jerrett M, Malmqvist E, Sjöström C, Taj T, Vargas AM (2021) Air quality in Africa: public health implications. Annu Rev Public Health 1–22. https://doi.org/10.1146/annurev-publhealth-100119-113802

Aklilu A, Necha T (2018) Analysis of the spatial accessibility of Addis Ababa's light rail transit: the case of East–West Corridor. Urban Rail Transit 4(1):35–48. https://doi.org/10.1007/s40864-018-0076-6

Amoatey P, Omidvarborna H, Baawain MS, Al-mamun A (2020) Evaluation of vehicular pollution levels using line source model for hot spots in Muscat, Oman. Environ Sci Pollut Res. https://doi.org/10.1007/s11356-020-09215-z

Bachtiar VS, Afrianita R, Mustofa I, Anugerah R (2020) Modeling and the validation model of PM10 concentration due to the changes in the dominant wind direction to the road in the roadside area. IOP Conf Series: Mater Sci Eng 846(1). https://doi.org/10.1088/1757-899X/846/1/012058

Caserini S, Pastorello C, Gaifami P, Ntziachristos L (2013) Impact of the dropping activity with vehicle age on air pollutant emissions. Atmos Pollut Res 4(3):282–289. https://doi.org/10.5094/APR.2013.031

Dida GO, Lutta PO, Abuom PO, Mestrovic T, Anyona DN (2022) Factors predisposing women and children to indoor air pollution in rural villages, Western Kenya. Arch Public Health 1–13. https://doi.org/10.1186/s13690-022-00791-9

Fekadu Y (2017) Contribution of vehicle exhausts gas emissions to the traffic air pollution of selected areas of Addis Ababa City. Addis Ababa University

Gibson MD (2013) A tm spheric P ollution plume air dispersion model. Atmos Pollut Res 4(2):157–167. https://doi.org/10.5094/APR.2013.016

Goyal U, Dhir AG (2015) Comparison of dispersion models in the assessment of air quality due to vehicular emissions. Environ Sci. https://api.semanticscholar.org/CorpusID:132183066

Gulia S, Nagendra S, Khare M (2015) Comparative evaluation of air quality dispersion models for PM2 5 at air quality control regions in Indian and UK cities. MAPAN. https://doi.org/10.1007/s12647-015-0149-x

Habtamu (2020) Determinants of youths rural to urban migration in Ethiopia (case of Addis Ababa) 2(15), 5–7

Haslina S, Shafie M, Mahmud M, Mohamad S, Lita N, Rameli F (2022) Influence of urban air pollution on the population in the Klang Valley, Malaysia: a spatial approach. Ecol Process. https://doi.org/10.1186/s13717-021-00342-0

Kebede L, Tulu GS, Lisinge RT (2022) Diesel-fueled public transport vehicles and air pollution in Addis Ababa, Ethiopia: effects of vehicle size, age and kilometers travelled. Atmos Environ: X 13:100144. https://doi.org/10.1016/j.aeaoa.2021.100144

Kerr LA, Goethel DR, Methods I, Edition S (2014) Simulation modeling as a tool for synthesis of stock identification information chemical imaging in food authentication

Kumar R, Shukla A, Parida M, Pandey G (2016) Urban roadside monitoring and prediction of CO, NO 2 and SO 2 dispersion from on-road vehicles in megacity Delhi. Transport Res Part D 46(2):157–165. https://doi.org/10.1016/j.trd.2016.03.019

Kume A, Charles K, Berehane Y, Anders E, Ali A (2010) Magnitude and variation of traffic air pollution as measured by CO in the City of Addis Ababa Ethiopia. Ethiop J Health Dev 24(3):156–166

Kumie A, Worku A, Tazu Z, Tefera W, Asfaw A, Boja G, Mekashu M, Siraw D, Teferra S, Zacharias K, Patz J, Samet J, Berhane K (2021) Fine particulate pollution concentration in Addis Ababa exceeds the WHO guideline value: results of 3 years of continuous monitoring and health impact assessment. Environ Epidemiol 5(3):1–9. https://doi.org/10.1097/EE9.0000000000000155

Lin C, Gillespie J, Schuder MD, Duberstein W, Beverland IJ, Heal MR (2015) Evaluation and calibration of Aeroqual series 500 portable gas sensors for accurate measurement of ambient ozone and nitrogen dioxide. Atmos Environ 100(2):111–116. https://doi.org/10.1016/j.atmosenv.2014.11.002

McKercher GR, Salmond JA, Vanos JK (2017) Characteristics and applications of small, portable gaseous air pollution monitors. Environ Pollut 223:102–110

Mehrdad (2013) Mathematical modeling considering air pollution of transportation: an urban environmental planning, case study in Petaling Jaya, Malaysia. J Chem Inf Model 53(9):1689–1699. https://doi.org/10.1017/CBO9781107415324.004

Milando CW, Batterman SA (2018) Sensitivity analysis of the near-road dispersion model RLINE - an evaluation at Detroit, Michigan. Atmos Environ 181:135–144. https://doi.org/10.1016/j.atmosenv.2018.03.009

Nieuwenhuijsen MJ (2016) Urban and transport planning , environmental exposures and health-new concepts , methods and tools to improve health in cities. Environ Health 15(Suppl 1). https://doi.org/10.1186/s12940-016-0108-1

Obanya HE, Nnamdi H, Togunde O (2018) Air pollution monitoring around residential and transportation sector locations in Lagos Mainland. J Health Pollut 8(19):1–10. https://doi.org/10.5696/2156-9614-8.19.180903

Onat B (2016) Modeling of PM10 dispersion in Rize City Center. 1st International Black Sea Congress on Environmental Sciences (Ibcess), 1(December). https://www.researchgate.net/publication/311909983

Piqueras P, Vizenor A (2016) The rapidly growing death toll attributed to air pollution: a global responsibility, pp 1–4

Singh A, Ng D, Gatari MJ, Kidane AW, Alemu ZA, Derrick N (2021) Air quality assessment in three East African cities using calibrated low-cost sensors with a focus on road-based hotspots. Environ Res Commun 3(075007):14. https://doi.org/10.1088/2515-7620/ac0e0a

Takuchev N, Vasileva I, Petrova S (2014) Dispersion modeling of the air pollution, emitted by the traffic in the transport tunnel under the old town of Plovdiv, Bulgaria. Ecologia Balkanica 6(1):1–15. https://www.researchgate.net/publication/266938288%0ADispersion

UN (2017) Addis Ababa City structure plan. In AACPPO. https://c40-production-images.s3.amazonaws.com

US EPA (2003) AERMOD: latest features and evaluation AERMOD : United States Environmental Protection Agency 454(3):1–41

US EPA (2015) User's Guide for the AMS/EPA Regulatory Model (AERMOD). Acta Universitatis Agriculturae et Silviculturae Mendelianae Brunensis 53(9):1689–1699 http://publications.lib.chalmers.se/records/fulltext/245180/245180.pdf%0Ahttps://hdl.handle.net/20.500.12380/245180%0Ahttp://dx.doi.org/10.1016/j.jsames.2011.03.003%0A10.1016/j.gr.2017.08.001%0Ahttp://dx.doi.org/10.1016/j.precamres.2014.12

Wang G, Van Den Bosch FHM, Kuffer M (2008) Modeling urban traffic air pollution dispersion, pp 153–158

Wei T, Zhai W, Wen D, Xiang S (2016) Comparison of measured and predicted ultrafine particulate concentration using CALINE4 and AERMOD models. Ecologia Balkanica 6(1). https://www.researchgate.net/publication/266938288

Wondifraw B (2019) Estimation of exhaust emission from road transport using COPERT software. https://doi.org/10.13140/RG.2.2.14593.71529